Periodic Gonadal Activity and Protracted Mating in Elasmobranch Fishes

KAREN P. MARUSKA, ELIZABETH G. COWIE, AND TIMOTHY C. TRICAS
*Department of Biological Sciences, Florida Institute of Technology,
Melbourne, Florida 32901-6988*

ABSTRACT   Temporal patterns of gonad development are determined by environmental cues that regulate hormonal cycles and ultimately affect a population's mating system. Annual periodicity of gonad histology is essentially unknown for the more than 450 species of batoid elasmobranchs. Temporal periodicity in spermatogenic activity and ova production in the Atlantic stingray (*Dasyatis sabina*) were examined by histology over a consecutive 20 month period. Gonadosomatic index (GSI) shows three distinct phases associated with structural changes at the cellular level. Testes in the *inactive phase* occur from March through July, have a low GSI, and are represented only by germinal (SI) and early spermatocyst (SII) stages. The *enlargement phase* begins in mid-August, followed by rapid testicular growth that peaks in October. Testicular recrudescence is characterized by a decline in the proportion of early stage spermatocysts (SI, II) and a sequential maturation of cells to the spermatocyte (SIII), spermatid (SIV), immature sperm (SV), and mature spermatozoa (SVI) stages. The measure of absolute spermatogenic production (ASP) is maximum from about August through January. The *diminution phase* is characterized by a decrease in male GSI from October through April associated with a reduced tissue biomass and predominance of early spermatogenic stages. The annual succession of peaks in sperm formation indicates continuous spermatogenesis through the fall–winter and shows that peak sperm production lags maximum GSI by approximately 3–4 months. Further, seminal vesicle diameter peaks in February, which also lags maximum GSI by 4 months. Egg growth in females is a periodic process of 5–6 months duration that involves vitellogenesis of 2–4 oocytes. Maximum ova diameter increases after mid-September, peaks in March ($\bar{x}$ = 10.62 mm), and covaries with the increase in female GSI. Despite the brief period of ovulation and fertilization in March–April, fresh mating scars and sperm in the lower reproductive tract of females confirm a protracted mating period from October through April–May. Thus, mating begins in the population at least 7 months prior to ovulation and fertilization. Current evidence indicates this protracted mating period is not explained by female sperm storage or arrested embryonic development. We suggest the protracted mating period serves some currently undetermined function such as induction of steroidogenesis, oocyte growth, or ovulation in females.   © 1996 Wiley-Liss, Inc.

Elasmobranch fishes show a wide range of reproductive strategies which reflect a diversity of morphological and physiological specializations such as internal fertilization and aplacental viviparity (Matthews, '50; Babel, '67; Pratt, '88; Gilmore, '93). However, there is only limited information available on seasonal cycles of gonad development and how they relate to the timing of reproductive events in the wild population. General reproductive periodicity strategies in elasmobranchs were first classified by Wourms ('77) and further characterized in males based on the relationship between relative gonad size as a gonadosomatic index (GSI) and mating season (Parsons and Grier, '92). The majority of information on elasmobranch temporal cycles addresses changes in oogenesis and steroidogenesis (e.g., Dodd, '72;

Craik, '78; Sumpter and Dodd, '79), while few studies concern spermatogenic activity in males. The broad categorizations of male cyclicity are supported by documentation of temporal spermatogenic variations in only a few shark species [e.g., *Squalus acanthias* (Simpson and Wardle, '67), *Scyliorhinus canicula* (Dobson, '74), *Mustelus manazo* and *Mustelus griseus* (Teshima, '81), and *Sphyrna tiburo* (Parsons and Grier, '92)] and some batoids [e.g., *Urolophus halleri* (Babel, '67) and *Dasyatis sabina* (Lewis, '82)]. Almost nothing is known about temporal development patterns of

---

gonadal tissues in the more than 450 batoid elasmobranch species, and no study has quantified periodic changes in spermatogenesis across the reproductive season. Such information is crucial to interpretation of the evolution of mating systems, associated endocrinological cycles, and regulation of reproductive activity in elasmobranch fishes.

Information on elasmobranch reproduction is largely descriptive and tissue development during reproductive activity remains essentially undescribed for the vast majority of species. Many studies rely heavily on the GSI to determine reproductive activity (Parsons, '82; Snelson, '89; Di Giacomo, '94). An assumption of this technique is that relative gonad size and reproductive readiness are positively correlated. However, the few studies that examined elasmobranch gonadal development at the tissue level do not support this assumption (Teshima, '81; Parsons and Grier, '92). Gonadosomatic index is useful to show changes in testicular size but does not provide an estimate of mating activity or reproductive readiness illustrated by histology. As a result, information on functional breeding season and gonadal activity in elasmobranchs is very limited. Further, histological changes in gonad structure must be determined for a species before proximate causal factors such as the action of sex steroids upon reproductive activity and periodicity can be determined.

The Atlantic stingray (Dasyatis sabina) is perhaps the most abundant and geographically dispersed elasmobranch in southeastern estuarine waters of the United States. Snelson et al. ('88) used macroscopic features in D. sabina from central Florida to conclude that mating occurs from October through April but ovulation and fertilization only in March–April. If correct, this remarkable observation of a protracted 7-month mating period but narrow 1-month window for ovulation and fertilization could represent a novel function for mating behavior in elasmobranch fishes. Our goal was to quantitatively confirm cyclicity of gonad tissue development, ovulation, and fertilization in relation to the mating behavior in a single population of D. sabina.

This study provides the first quantified histological analysis of temporal changes in spermatogenesis and ova production in a batoid elasmobranch, and demonstrates that the GSI is an inadequate measure of reproductive activity in this and probably other batoid species. We also demonstrate differences in the duration of reproductive readiness between male and female rays and the existence of a protracted 7 month

mating period. Three separate hypotheses to explain this protracted mating period are discussed: (1) female sperm storage, (2) arrested development, and (3) reproductive induction. We suggest this extended mating period likely serves some undetermined function such as induction of steroidogenesis, oocyte growth or ovulation in females, or possibly a combination of several reproductive phenomena.

MATERIALS AND METHODS

Collections

Ten mature Atlantic stingrays of each sex (male > 19 cm disc width, female > 22 cm disc width) were collected on or near the 15th of every month from July 1993 through February 1995. Rays were sampled at the same geographical location near the southern end of the Banana River on the east coast of central Florida (Cook, '94). Disc width (DW) and length of each animal was measured to the nearest millimeter and total weight to the nearest milligram. Livers and reproductive organs were removed, blot dried, and weighed to the nearest milligram on an electronic balance. Gonads were preserved in 10% formalin (in a 1:10 ratio) and stored in 50% iso-propyl alcohol. Male and female GSI and hepatosomatic index (HSI) were determined as [(gonad weight/total body weight) × 100] and [(liver weight/total body weight) × 100], respectively. The epigonal organ was included in both male and female GSI measurements due to its close association with the reproductive tissue. Most elasmobranch GSI studies do not mention epigonal tissue inclusion or removal and it is undocumented whether a seasonal periodicity of this organ covaries with that of the gonadal tissues.

Histology

A single 2–3 mm thick segment of the gonad was removed from the center of each testis or left ovary. Tissue samples were dehydrated in a graded ethanol series (70–100%), cleared in toluene, and infiltrated in a series of toluene:paraffin (2:1, 1:1, 1:2) and 100% paraffin baths on an Autotechnicon. The use of small gonad segments and increased dehydration and infiltration times (7 hr each) maximized the penetration of wax into the tissue for improved section quality. Paraffin blocks were sectioned at 8–10 μm on a sliding microtome, mounted on chrom-alum coated slides, and stained with Mayer's Hematoxylin and Eosin (Humason,'79).

Ovary anatomy

The ovaries of six female stingrays per month were examined macroscopically for 20 consecutive months (July 1993–February 1995). The six largest eggs were removed from the left ovary, blot dried, weighed to the nearest milligram, and diameters measured to the nearest millimeter with dial calipers. Mean oocyte diameter was calculated for each individual to examine temporal changes in egg size. Several ovaries were examined by histology as described above to verify mature vs. immature oocytes and the overall morphology of the ovary. Cloacal, uterine, or nidamental gland swabs were taken monthly from six mature females from November 1994 through October 1995. Fluid was removed with sterile scalpel blades, smeared on chrom-alum coated slides, dried, and stained with 0.3% Wright's stain in methanol to visualize spermatozoa.

Testis anatomy

Verification of uniform development throughout the testis was determined by preliminary analysis of tissue removed from a rostral, medial, and caudal portion of the gonad from six male stingrays within the same month (September 1994). No difference was found in the number of each spermatocyst stage represented between the three areas ($X^2 = 3.43$, df = 10, $P = 0.97$). Consequently, all sections were taken from the central portion of a single lobe in the medial area of the testis and represent general development patterns of the gonad tissue.

Histological sections were examined for six male rays per month for 20 consecutive months (July 1993–February 1995) to quantify seasonal changes in testicular structure. One representative full lobe cross section from each animal was analyzed by light microscopy. Primary zone was calculated as a percentage of each total field on the transect line. Counts of spermatocysts (which represent each of the seven identified stages of spermatogenesis described below) were made within the circular field of view at 200x on a transect line from the section margin (advanced developmental stages) toward the primary zone or across to the opposite peripheral edge. Means ($\bar{x}$) and standard errors (SE) were computed for the six individuals per month, and each stage (stages II–VII) was converted to a percentage of the total cross-sectional area within the section. Photomicrographs of each spermatocyst stage were taken on a compound light microscope. Because the measure of cross-

sectional area may be independent of gonad size, we generated an absolute estimate of stage production. A measure of absolute spermatogenic production (ASP) was calculated as: $ASP_i = p_i m$, where p = proportion of gonadal cross-sectional area, m = gonad mass, and i = developmental stage of spermatogenesis (SI–SVII). The ASP provides an assessment of the absolute contribution of each developmental stage to total sperm production, which integrates monthly differences in gonad size. Seminal vesicle diameters were measured to the nearest millimeter for six male rays per month for 20 consecutive months (July 1993–February 1995). Measurements were taken from a medial coil in the left seminal vesicle on each animal. Sperm presence in enlarged vesicles was verified under a microscope but not quantified.

RESULTS

Male gonad anatomy and histology

Testis morphology

The testes of the Atlantic stingray are paired, dorsoventrally flattened organs located in the anterior peritoneal cavity suspended from the dorsal wall by mesorchia (Fig. 1A). Both testes are well developed and functional but the right testis is reduced in size, probably due to the placement of the large ipsilateral spiracular intestine and stomach. The organs are supported on the posteriolateral margin by the highly vascularized epigonal organ. Relative proportion of the testis and epigonal organ varies over time, with testicular tissue dominant from September through April and epigonal from May through August, but this was not quantified due to the difficult separation of these tissues. Each testis is an aggregation of irregular lobes that project inward from the testicular appendage at the gonad surface. Each lobe contains spermatocysts in various stages of spermatogenesis which develop and migrate radially to the periphery of the lobe, characteristic of the compound structured testis described by Pratt ('88). Mature sperm then pass to collecting ducts at the lobe periphery and through the vas efferens to the epididymis. Sperm continues through the vas deferens and Leydig's gland to the seminal vesicles for storage. At copulation, this sperm is passed to the female via the clasper organs.

Histological stages

Histological analysis of the testis shows distinct structural spermatocyst stages that change over time. We follow the general terminology used to
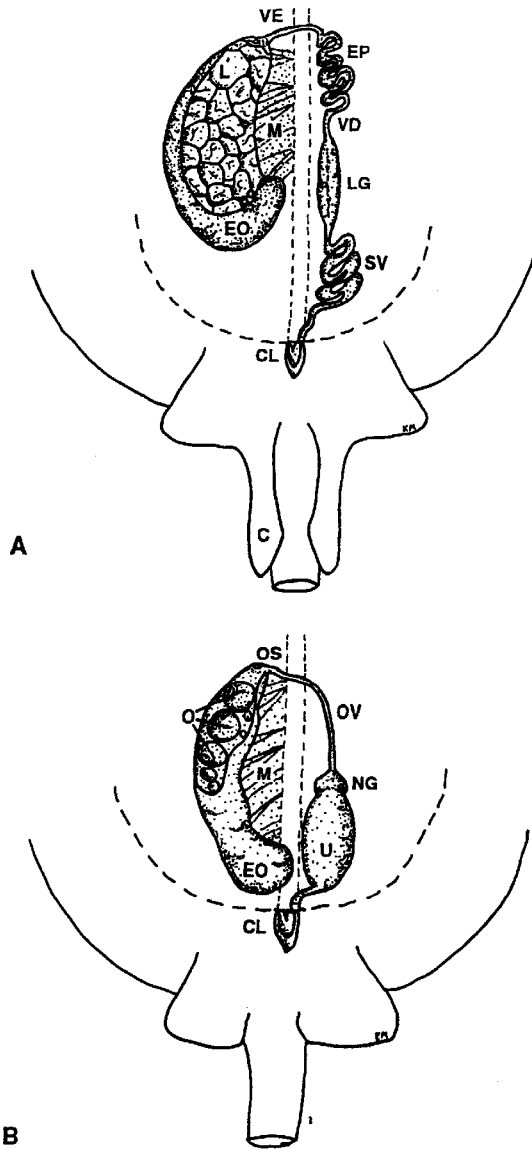
Fig. 1. Reproductive anatomy of the mature Atlantic stingray (*Dasyatis sabina*), ventral view. A: Testicular lobes (L) of males are in close association with the epigonal organ (EO). Mature sperm leave the testis via the vas efferens (VE) and pass to accessory reproductive structures composed of the highly coiled epididymis (EP), vas deferens (VD), Leydig's gland (LG), and seminal vesicles (SV). Sperm is then transferred to the female during copulation via the clasper organs (C). B: Female ovaries contain many oocytes (O) of various diameters. The ovary is closely associated with the highly vascularized epigonal organ (EO). Mature oocytes are released from the ovarian surface to the ostium (OS) and travel through the oviduct (OV) to the nidamental gland (NG). Eggs are fertilized at the nidamental gland and then enter the

TABLE 1. *Summary of cell and spermatocyst diameters in the testis of* D. sabina[1]

	Diameter (μm)	
	Mean ± SD	Range
Germ Cells	4.1 ± 1.1	3.6–7.2
Spermatogonia	11.8 ± 2.4	7.2–18.0
Spermatocytes	7.4 ± 1.0	6.0–10.8
Spermatids	3.6 ± 0.5	2.4–4.8
Sperm head length	28.6 ± 3.5	21.6–36.0
SII	54.7 ± 15.1	21.0–98.0
SIII	120.8 ± 22.1	63.0–175.0
SIV	136.5 ± 31.9	84.0–203.0
SV	133.6 ± 22.7	84.0–182.0
SVI	117.0 ± 20.2	84.0–161.0
Sertoli cells		
SI	4.6 ± 0.4	2.4–6.0
SII	5.4 ± 0.2	3.6–7.2
SIII	7.1 ± 0.3	4.8–7.2
SIV	7.7 ± 1.3	4.8–13.2
SV	9.3 ± 0.4	6.0–14.4
SVI	8.7 ± 1.8	5.4–12.6

[1]Each statistic was computed for 10 measurements sampled from each of six fish (n = 60).

describe male gamete production in the bonnethead shark (Parsons and Grier, '92) and the functional unit of spermatogenesis as the basement membrane-bound spermatocyst (Grier, '92). Gonad development is characterized by cell differentiation associated with changes in spermatocyst composition and diameter (Fig. 2A). Spermatocyst diameter across developmental stages and general cell type diameters are summarized in Table 1.

Stage I (SI): primary or germinal zone. Spermatogenesis initiates at the primary or germinal zone prior to the formation of a structured membrane-bound spermatocyst. The primary zone shown in Figure 2B contains loosely organized germ cells approximately 4.1 μm in diameter and larger primary spermatogonial cells about 11.8 μm in diameter. Clusters of spermatogonia are also associated with putative Sertoli cell nuclei (4.6 μm diameter), but a true germinal epithelium does not yet exist. Spermatogonia contact interstitial tissue and the circular basement membrane-bound spermatocyst is unformed. Spermatogenesis initiates at the testicular appendage in the center of each lobe as described for the round stingray, *Urolophus* (Babel, '67). Primary spermatogonia and putative

uterus (U) for development. Only the right testis and ovary are shown and gonads are displaced to the right side of the peritoneal cavity to show underlying structures. Mesorchia (M) suspends the gonadal tissue in the peritoneal cavity. Dashed midline represents the vertebral column. CL = cloaca.
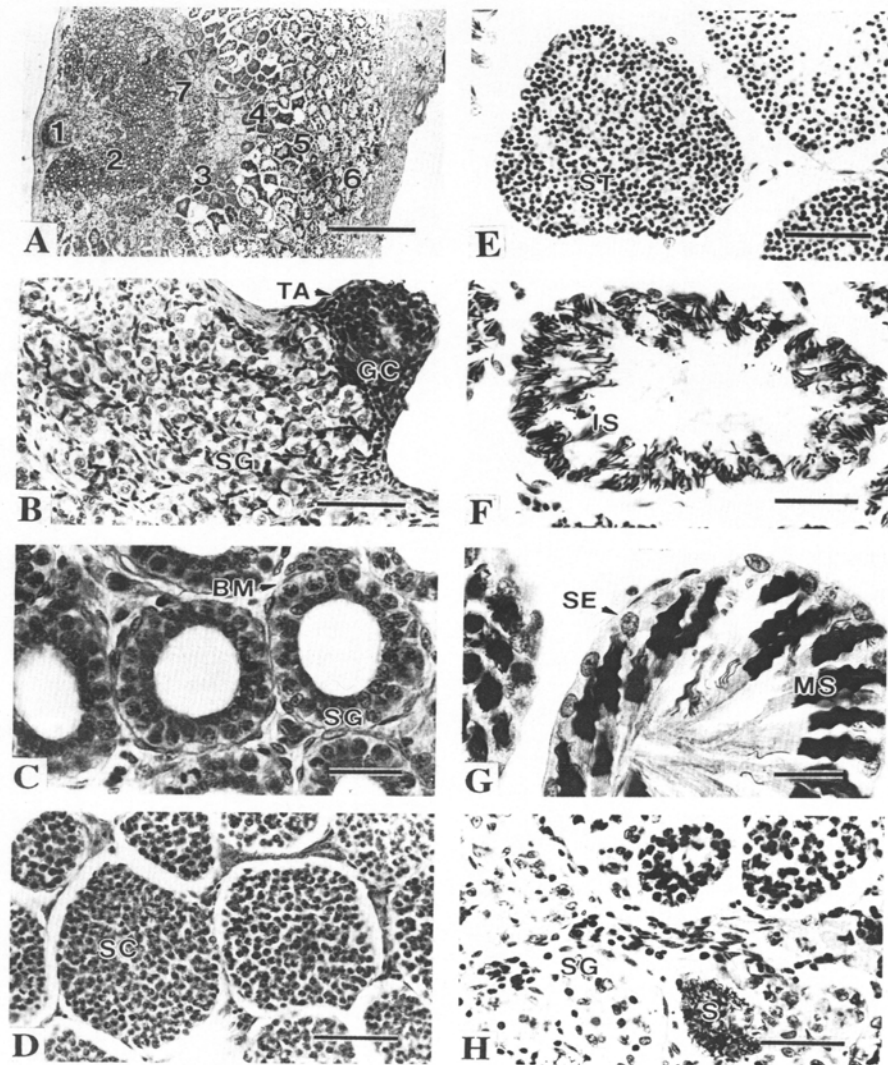
Fig. 2. Histological sections from male *D. sabina* testes taken at representative times during the reproductive cycle. **A:** Histological cross section through a single testicular lobe that shows the seven identified stages of spermatogenesis. Stages I–VII are labeled as the Arabic numerals 1–7, respectively. Bar = 0.5 mm. **B:** Stage I (1) contains the testicular appendage (TA) with associated germ cells (GC) and primary spermatogonia (SG). Bar = 50 μm. **C:** Stage II (2) early spermatocysts show layers of spermatogonial cells (SG) enclosed by a basement membrane (BM). Bar = 25 μm. **D:** Stage III (3) spermatocysts contain spermatocytes (SC) that fill the spermatocyst lumen with monomorphic spherical cells. Bar = 50 μm. **E:** Stage IV (4) spermatocysts show spermatids (ST) with spherical to elliptical nuclei that result from the second meiotic division. Bar = 50 μm. **F:** Spermatids undergo spermiogenesis to form unorganized immature sperm (IS) characteristic of stage V (5) spermatocysts. Bar = 50 μm. **G:** Stage VI (6) spermatocysts are characterized by mature sperm that have completed the maturation process and are organized into cone-shaped packets (or spermatozeugmata) associated with Sertoli cells (SE). Bar = 25 μm. **H:** The degenerate zone (7) contains flattened spermatocysts at the primary zone margin that result from the breakdown of spermatogonia (SG). Unreleased and undegraded sperm (S) is often seen adjacent to the degenerate zone. Bar = 50 μm.

Sertoli cells aggregate around the testicular appendage, begin to divide, and migrate radially away from the appendage. Clusters of spermatogonia are separated by genital cords that develop into testicular ducts in this area, as described by Grier ('93). The primary or germinal zone was not described as a discrete stage in the bonnethead shark by Parsons and Grier ('92).

Stage II (SII): early spermatocysts. Early spermatocysts (55.0 μm diameter) form when spermatogonia and Sertoli cells divide, descend into the lobe, and are enclosed by a basement membrane (Fig. 2C). Newly formed spermatocysts contain a peripheral layer of spermatogonia and an inner layer of Sertoli cells that surround a hollow lumen. Spermatocysts mature and increase in diameter (range = 21.0–98.0 μm) as the spermatogonia divide and form 2–6 layers of cells. Sertoli cells migrate to the periphery of the spermatocyst when 3–4 layers of spermatogonia are formed. In contrast to Parsons and Grier ('92), we include all spermatocysts with secondary spermatogonia in this single stage rather than two.

Stage III (SIII): spermatocytes. Sertoli cells (now 7 μm in diameter) migrate to the periphery of the spermatocyst. Spermatogonia complete mitosis, enlarge, and begin meiosis to form primary spermatocytes (Fig. 2D). Primary spermatocytes entirely fill the membrane-bound spermatocyst with monomorphic spherical cells approximately 7.4 μm in diameter. Primary spermatocytes complete the first meiotic division to become smaller secondary spermatocytes. Both primary and secondary spermatocytes are included in this stage due to the brief first meiotic division and their similar appearance, which differs from Parsons and Grier ('92) who separated spermatocytes into two classes. Furthermore, spermatocysts with either primary or secondary spermatocytes have a larger diameter (121.0 μm) than those of early spermatocysts (SII) (55.0 μm) and are often mixed with later stage spermatocysts.

Stage IV (SIV): spermatids. Spermatids result from the second meiotic division of secondary spermatocytes (Fig. 2E). Spermatids completely fill the spermatocyst, are smaller (3.6 μm) than spermatocytes (7.4 μm), and have spherical nuclei. Newly formed spermatocysts in this stage have an occluded primary lumen while later spermatocysts begin to develop a secondary lumen. Spermatocysts increase in diameter (136.5 μm) from those of the previous stage (121.0 μm), and possess dark-stained cells of equal size. Spermatids near the start of spermiogenesis contain elliptical nuclei.

Spermatocysts develop and migrate toward the lobe periphery, with a mix between SIII and SIV stages. Absence of a clear demarcation line between stages is presumably due to different rates of differentiation or migration through the tissue or angle of the section.

Stage V (SV): immature sperm. Spermatids undergo maturation via spermiogenesis, which involves differentiation of the sperm head, midpiece, and tail. Individual sperm nuclei associate with Sertoli cells but are separate and unorganized (Fig. 2F). Sertoli cells are large at this stage (9 μm diameter) and positioned at the spermatocyst periphery. The diameter of spermatocysts with immature sperm (133.5 μm) remains about the same as those of the previous spermatid stage (136.5 μm). Adjacent spermatocysts routinely possess spermatids in asynchronous phases of spermiogenesis, possibly due to differential development or migration rates. Immature sperm in late stages of development are radially oriented with tails in the lumen but are not organized into clumps.

Stage VI (SVI): mature spermatocyst. Sperm complete the maturation process and organize into tight cone-shaped packets (Fig. 2G) described as unencapsulated masses of naked sperm, or spermatozeugmata (Pratt and Tanaka, '94). Sperm heads have a spiral morphology, are oriented toward the periphery of the spermatocyst and embedded in the apical regions of Sertoli cells. A single Sertoli cell (9 μm diameter) is associated with each packet, which ruptures to initiate sperm release (=spermiation) from the spermatocyst. Mature spermatocysts (117.0 μm diameter) are reduced in diameter from immature spermatocysts (133.5 μm diameter). Mature spermatocysts are located only at the lobe periphery in close proximity to the collecting ducts, but may be intermixed with spermatocysts which contain immature sperm in latter stages of development.

Stage VII (SVII): degenerate zone. The degenerate zone results from the breakdown of spermatogonia once development begins to wane. Spermatocysts appear flattened and empty, with ruptured Sertoli cells that congregate at the primary zone margin (Fig. 2H). Spermatogenesis has ceased with no new formation of spermatocysts. Spermatocysts that recently ruptured to release mature sperm may have free sperm scattered among the other spermatocysts. Unreleased and undegraded mature sperm are also often seen adjacent to the degenerate zone.

Temporal periodicity

Male testicular and hepatic tissues demonstrate distinct annual changes in gross morphology. Testes from April through August are poorly developed, with indistinct testicular lobes and minimum GSI values (Fig. 3A). Testicular recrudescence begins after mid-August followed by an increase in GSI to maximum values in October. Testicular diminution follows this peak shown by the decline in GSI over subsequent months to minimum levels in June–July of both years (Fig. 3A). Male HSI shows a distinct temporal cycle across the same time period, minimum values in December–January, and maximum values in September of both years. The September HSI maximum occurs 1 month prior to that of GSI but follows the GSI diminution phase from mid-October through April (Fig. 3A).

Male accessory reproductive structures show variations in size and sperm content over time that do not covary with annual changes in gonad size. Seminal vesicle diameter begins to increase in August–September, peaks in February, then declines in size from March to July as the density of sperm packets decreases (Fig. 3B). The diameter of epididymis ducts follows a similar trend but was not quantified. Thus, sperm in the accessory structures peaks in February and lags maximum GSI by approximately 4 months.

Male rays show distinct temporal changes in testis structure and development at the cellular level. The ASP shows absolute contribution of each stage to the final production of sperm and in most stages covaries with the percent area in each month (Fig. 4). The percentage of primary zone (SI) present in the fall months during peak testicular activity is reduced to less than 20% of the total cross-sectional area. This reduction is likely due to increased late stage spermatocysts in the tissue. Analysis of the ASP indicates that the primary zone is also reduced relative to previous months but remains a germ cell source throughout the annual cycle (Fig. 4). The greatest proportion of early spermatocysts (SII) in 1994 occurred in May–July (Fig. 4), but this is also when testis size is at the yearly minimum (Fig. 3A). In comparison, the largest SII biomass occurred in September–October of both 1993 and 1994, which coincides with maximum GSI and shows the largest biomass for any cell stage. Thus, the SIII peak in October–November followed by a decline in early spermatocysts (SII) and subsequent increase in later stage spermatocysts (SIII–

VI) is due to maturation of SII cells (Fig. 4). These latter stages (SIV–VII) peak in succession over subsequent months. Mature sperm (SVI) reach maximum values in January of 1994 and in October of 1994, shown by ASP. However, GSI values after October 1994 decline much quicker than those in 1993, which may account for the shift in ASP values to October of the same year. Further, the April 1994 peaks in percent area for stages IV–VI occur when testicular size is small. Analysis of ASP indicates the contribution of these stages for sperm production is minimal because testicular biomass is low. The degenerate zone reaches a maximum value in March 1994, which illustrates the breakdown of spermatocysts and the end of spermatogenic activity. To summarize, spermatogenesis in the Atlantic stingray begins in July–August, illustrated by the decline in SI and SII spermatocysts and coincident increase in SIII followed by latter stages. Sperm production proceeds through January and is followed by a wane in activity in February–March that lasts through the summer months.

Female gonad anatomy

Ovary morphology

The ovaries are paired, elongate organs suspended from the peritoneal cavity by mesorchia and supported by the epigonal organ on the posteriolateral margin (Fig. 1B). Unlike males, only the left organ is functional and produces viable ova. The right ovary is reduced in size, composed primarily of epigonal tissue, and does not release ova. The ovaries of mature stingrays contain many small oocytes embedded in connective tissue throughout the year. At the onset of ova maturation in October–November, several oocytes begin to develop and grow until release at ovulation in March–April. Ovaries in the several months prior to ovulation routinely contain 2–4 large mature ova ($\bar{x}$ range = 6–10 mm) at the anterior surface, with many smaller immature oocytes ($\bar{x}$ range = 2–5 mm) beneath. The largest mature ova are released from the ovary to the ostium and oviduct, while other mature eggs migrate to the periphery and external ovarian surface.

Temporal periodicity

The only apparent gross morphological change in the ovary is the annual production and development of ova. At the October onset of ova maturation and vitellogenesis eggs increase in size, become yellow/orange in color, and epigonal tissue is less obvious in sections. GSI shows a steady
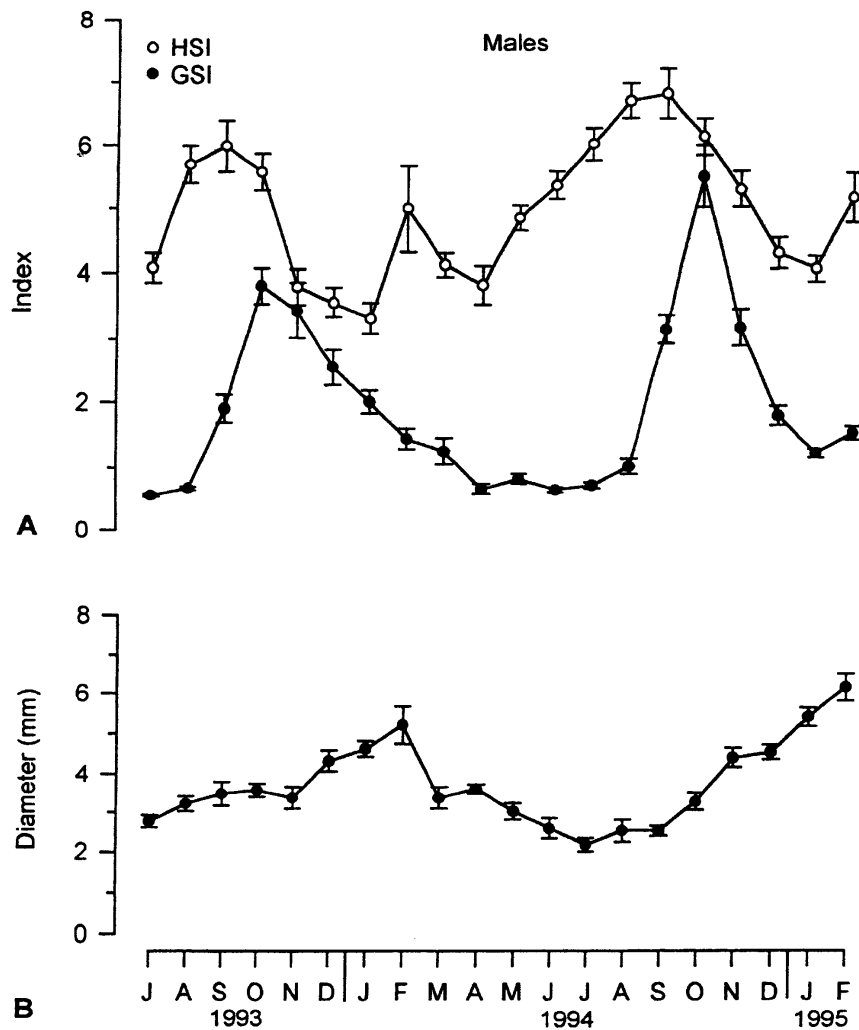
Fig. 3. **A:** Male gonadosomatic index (closed circles) and hepatosomatic index (open circles) for *D. sabina* collected over 20 consecutive months (July 1993–February 1995). Each point represents the mean ± SE of 10 animals. Male GSI and HSI both show distinct temporal periodicity with maximum HSI values (September) about 1 month prior to maximum GSI values (October). **B:** Annual periodicity of seminal vesicle di-

ameters measured in six rays per month for the same period. Data are expressed as a mean ± SE. Seminal vesicle diameter begins to increase in about September, reaches a peak in February, and declines over subsequent months. Seminal vesicle periodicity lags peak GSI values by 4 months and female ovulation by 1 month.

increase after October 1993 and a maximum in February–March 1994 (Fig. 5). The increase in gonad size corresponds to the maturation of oocytes (described below) within the ovary, and temporal fluctuations in GSI follow that of ova diameter. Between mid-May and mid-September the left ovary is small in size, contains many small immature oocytes embedded in connective tissue, and epigonal tissue is predominant in histologi-

cal sections. A decrease in ovary size to a minimum value of 0.5–0.7% of body weight from June through September 1994 is followed by the increase in relative ovary size, as observed in the previous year.

Female HSI was calculated over the study period to examine covariance in relative gonad and liver size with ovarian development. Unlike males, liver size shows no clear temporal periodicity in
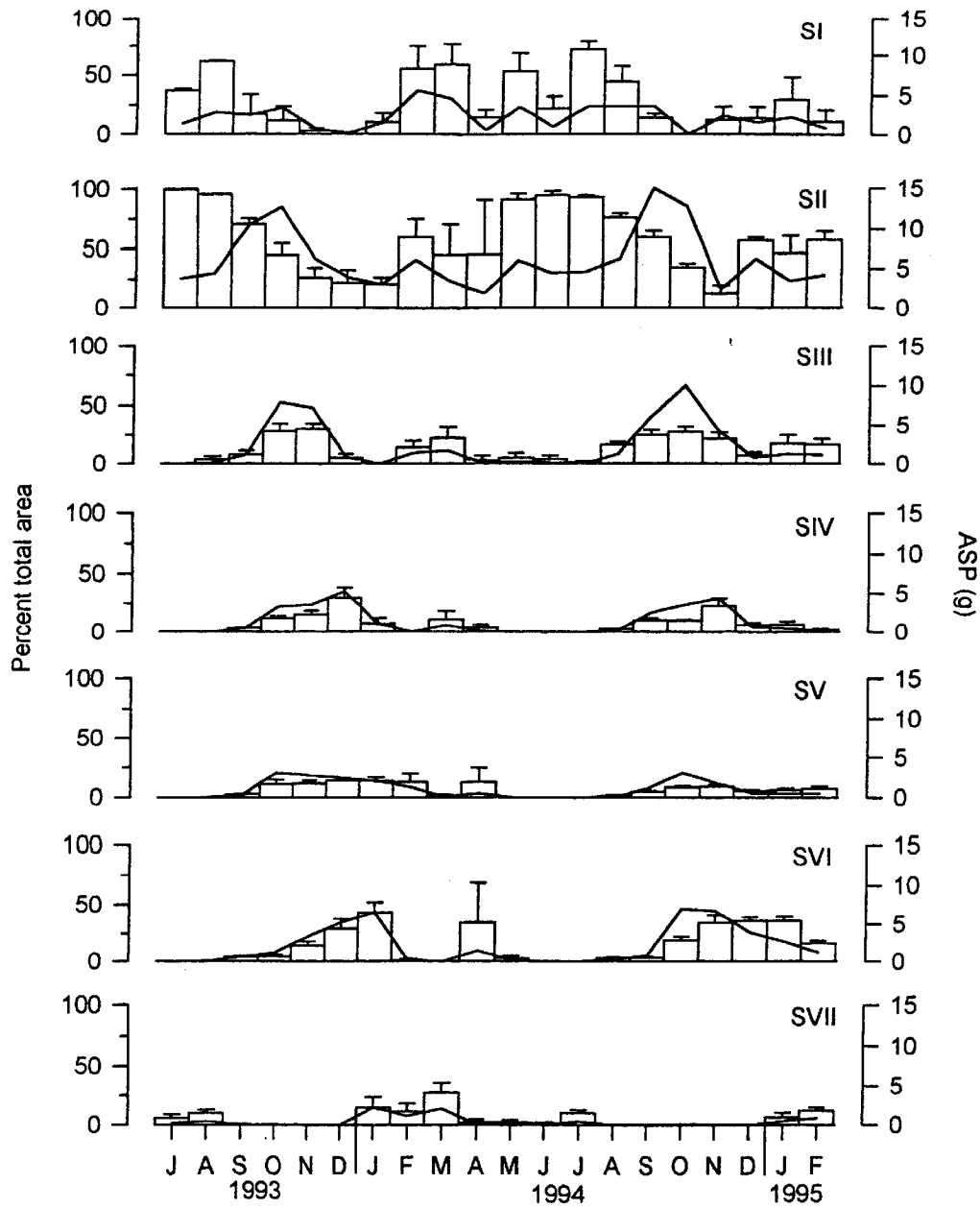
Fig. 4. Periodicity in spermatogenesis stages of *D. sabina* testes collected from July 1993 to February 1995. Primary zone was calculated as a percentage of each field along the tissue transect. Stages II–VII were expressed as a mean percent total area ± SE of each spermatocyst stage in a single testicular lobe cross section from six individuals per month. Stages are primary zone (SI), early spermatocyst (SII), spermatocytes (SIII), spermatids (SIV), immature sperm (SV), mature sperm (SVI), and degenerate zone (SVII). Line plot shows periodicity in the ASP for each stage within each month. The primary zone (SI) is present in almost every month and provides germ cells for each annual spermatogenic cycle. The largest biomass of SII occurs in September–October followed by maturation of these spermatocysts through stages III–VII over subsequent months. Spermatogenesis is dominant from about July–August through January.
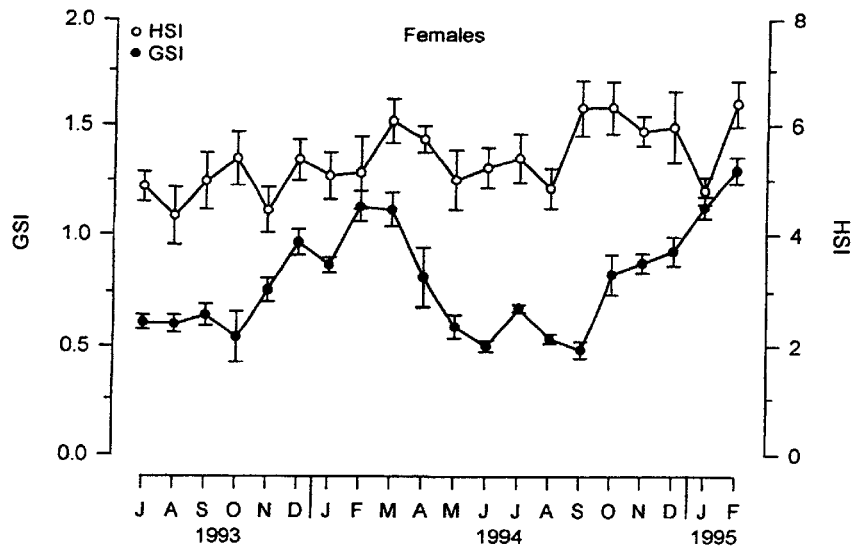
Fig. 5. Female gonadosomatic index (closed circles) and hepatosomatic index (open circles) for *D. sabina* collected monthly from July 1993 to February 1995. Each point represents the mean ± SE of 10 animals. GSI shows a steady increase after October to maximum values in February–March, which covaries with ova diameter. Unlike males, female liver size shows no clear temporal periodicity across years.

females (Fig. 5). Maximum average HSI occurs in September 1994 ($\bar{x}$ = 6.83 ± 0.39 SE mm) but the high variability obscures any potential true monthly changes. No gravimetric evidence for decreases in liver size during the October–March 1994 period of egg enlargement was evident.

Egg development involves the enlargement of 2–4 ova that begins after mid-September and peaks in March 1994 ($\bar{x}$ = 10.62 ± 0.901 SE mm). The apparent decrease in egg size in mid-March results from both ovulated females with small residual oocytes and unovulated females, shown by the relatively large variance in April 1994 (Fig. 6). A second brief peak of lower magnitude in ova diameter ($\bar{x}$ = 6.02 ± 0.45 SE mm) occurred in July 1994, which corresponds to a brief low-magnitude peak in female GSI as well. However, no evidence for ovulation was observed at this time. Histological cross sections of ovaries verify that ova are present throughout the year and that the large diameter eggs are mature and filled with yolk granules.

Despite the distinct period of egg growth and relatively brief time window for ovulation, females mated for more than seven continuous months. Sperm were present in the cloaca, uterus, or nidamental glands of all females from November 1994 through February 1995 (Fig. 7). Sperm occurred in 80% of females in March, declined to less than 25% in April–May, and were absent from June to September 1995. Evidence for mating was again seen in 60% of females in October 1995 (Fig. 7). Sperm packets were never found in the uterus or nidamental gland, but mucoid sperm masses occurred in the cloaca of several females during March–April, indicative of a recent mating event. Ubiquitous presence of sperm in the lower female reproductive tract from October through April–
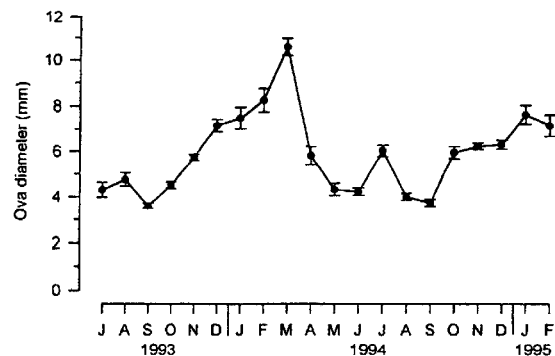
Fig. 6. Temporal periodicity in ova diameter for *D. sabina* females collected monthly from July 1993 to February 1995. Each data point represents the mean diameter ± SE of the six largest eggs measured in six individuals per month. Egg growth begins after mid-September and peaks in March, followed by a decline that indicates a brief time period of ovulation in March–April.
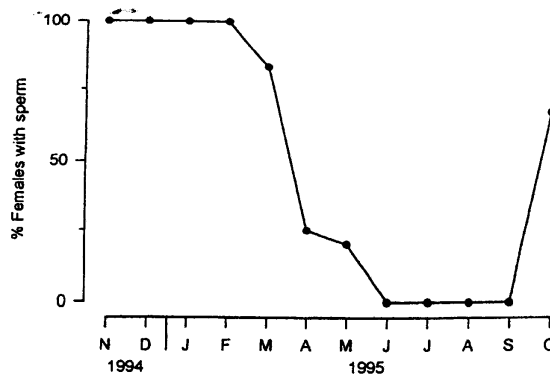
Fig. 7. Temporal fluctuations of sperm in the female reproductive tract from November 1994 through October 1995. Values represent the percentage of females with sperm in the reproductive tract from the total number of females examined per month (n = 6). Sperm are absent in females from June through September, and are present for the remainder of the year. These data along with observed scar patterns on females indicate a protracted 7 month mating period from October through April–May.

May indicates a protracted 7 month mating period in this population.

DISCUSSION

This study provides the first quantitative evidence of annual changes in testicular structure and spermatogenesis in a batoid elasmobranch (*Dasyatis sabina*). The temporal cycle of sperm production in the elasmobranch testes is evident by the distinct changes in the percent area and mass of each spermatogenic stage observed through histological analysis of this tissue. Parsons and Grier ('92) showed an annual pattern of development in the testes of the bonnethead shark (*Sphyrna tiburo*), by a distinct cycle in spermatocyst diameter correlated with stage of spermatogenesis. Similarly, spermatogenesis in the Atlantic stingray follows an annual cycle of spermatocyst formation and development but the proportion of different spermatocyst stages fluctuates throughout the year. Primary zone is present throughout the year and provides the germ cells necessary to initiate spermatogenesis each annual cycle. Early spermatocysts compose a large proportion of the gonad in summer months, but testes are small so the absolute spermatocyst production is minor. The largest biomass of SII occurs in September–October of both years followed by maturation of these spermatocysts through stages III–VII over subsequent months. The decrease in SII ASP in summer may represent testicular shrinkage in which active spermatogenesis has ceased and mature

sperm are passed to the accessory storage organs, leaving primarily SII cells within the testis. The seven stages of spermatocyst development reported in the present study are easy to identify, may be used to determine spermatogenic activity, and are a better predictor of activity in the elasmobranch testis than gross morphological data alone.

Sertoli cells within each spermatocyst stage also undergo a periodic development that begins with their association with spermatogonial cells (SI) and ends with released sperm via spermatocyst rupture (SVI–VII). Sertoli cell diameters increase as development proceeds from the primary zone stage (SI) to the mature sperm stage (SVI). However, ruptured spermatocysts degenerate so the germinal epithelium must be renewed each reproductive cycle as spermatocysts form in the primary zone (Grier, '93). The continual presence of primary zone in *D. sabina* supplies the new population of Sertoli and germ cells for each annual cycle necessary to initiate spermatogenesis at the onset of reproductive activity.

The annual HSI cycle in male *D. sabina* begins with an increase in liver weight in summer just prior to maximum GSI levels, followed by a decrease in fall and winter at the onset of mating. Similar fluctuations in male HSI are reported for the catshark, *S. canicula* (Craik, '78), and the school shark, *Galeorhinus galeus* (Peres and Vooren, '91). Our study population of *D. sabina* feeds heavily during the summer on ophiuroid discs, which are rich in gonads (Cook, '94). It is possible that this rich energy source is stored in the male liver to provide winter nutrient reserves for protracted sperm production and to compensate for possible reduced food abundance in cooler water or reduced feeding activity during the mating period. Further, estrogen production by the mature testis in certain elasmobranchs corresponds to increased HSI at sexual maturity (Craik, '78). The annual periodicity in biomass and cellular composition of testicular tissue that produces steroid hormones may explain the annual HSI cycle in the stingray. An examination of seasonal sex steroid concentrations in *D. sabina* and the role of liver reserves in sperm production is necessary to confirm the significance of the male HSI periodicity.

The absence of a decrease in female liver size during periods of egg growth indicates that liver reserves are not used exclusively as oocyte resources. Male and female rays feed on essentially the same food items throughout the year (Cook, '94), thus dietary differences cannot explain dif-

ferent seasonal patterns in liver mass. Variation in HSI of the catshark (Craik, '78) and school shark (Peres and Vooren, '91) is due to differential lipid deposition during the reproductive cycle rather than distinct vitellogenic activity. The HSI of female *D. sabina* may not show a decline during egg growth because lipids and proteins may be stored and processed continuously throughout the year without significant changes in biomass.

Gonadosomatic index is the most frequent method used to identify seasonal changes in testicular structure and to define mating seasons for shark populations (Parsons, '82; Snelson, '88, '89; Tanaka et al., '90; Abdel-Aziz, '94). Our work shows that this popular fisheries technique is useful to illustrate changes in testicular size but does not provide an estimate of mating activity. In *M. griseus, M. manazo*, and *S. tiburo*, male GSI peaks 6 months prior to the defined mating season when females do not ovulate (Teshima, '81; Parsons and Grier, '92). In male stingrays, GSI begins to increase in mid-August, reaches a maximum in October, and declines rapidly over subsequent months. Our histological analyses show mature sperm production is maximal from about July–August through January, when testes begin to decrease in relative size and are actually in the process of degeneration. Thus, histological analyses demonstrate that peak GSI is not correlated with peak sperm production, male reproductive readiness, or the mating period in *D. sabina*.

In addition, seminal vesicle size peaks 4 months after maximum GSI and 1 month prior to ovulation. This indicates that males store sperm for use after the end of spermatogenesis. The storage of sperm in the terminal ampulla of the epididymis is fairly common in male elasmobranchs and thought to be a strategy to ensure male reproductive success (Pratt and Tanaka, '94). Male *D. sabina* may produce large quantities of sperm during the winter and store it for a short time in the epididymis or seminal vesicles to ensure sperm availability when females are ready to ovulate in the spring. The condition of male accessory reproductive structures such as the seminal vesicles and epididymis may be a more accurate indicator of imminent fertilization than the traditional gonadosomatic index in species that lack a distinct but brief mating period.

Significance of protracted mating activity

The sequence of reproductive events in *D. sabina* can be summarized as follows: the presence of mating scars on the body and sperm in the female reproductive tract indicate a mating period of approximately 7 months, from October through April–May. Ovulation and fertilization occur in a narrow time window in March–April, with no evidence for a second ovulation. Gestation time is 3–4 months, with parturition in late June through early August. If both ovulation and fertilization occur in March–April, then why does mating activity begin 7 months prior? We discuss three hypotheses and briefly list several others that may explain this protracted mating period.

Female sperm storage hypothesis

Sperm storage occurs in females of every group of jawed vertebrates and allows the female to control fertilization and parturition to a time when environmental conditions are optimal for offspring survival (Howarth, '74). The nidamental (or oviducal) gland is proposed as the year-round sperm storage site in elasmobranchs (Metten, '44; Wourms, '77; Pratt, '93). Sperm may be stored loosely or in dense packets in the nidamental gland from weeks to even years in some shark species (Pratt, '93). Sperm occur in the nidamental gland of *D. sabina* only in March–April, immediately prior to ovulation. As a result, Lewis ('82) suggests the uterus as an alternate sperm storage site in this species. However, sperm in the dogfish (*S. caniculus*) are stored in the nidamental gland and those in the uterus are destroyed by the uterine lining (Metten, '44). Although uterine sperm degradation was not documented for *D. sabina*, the vaginal lining may resorb sperm (Lewis, '82). However, until uterine resorption of sperm is confirmed, it is possible that uterine sperm storage does exist. It is currently unknown whether there is a time-dependent relationship between copulation during the protracted mating period and fertilization (i.e., sperm competition). Furthermore, sperm storage is generally thought to be a strategy used in species that are nomadic or segregated by sex (Pratt, '93). Our study population of *D. sabina* does not seem to segregate by sex at any time of the year, which casts doubt on the female sperm storage hypothesis in this species but does warrant further investigation.

Arrested development hypothesis

Arrested development is a pause in embryonic development that follows mating and fertilization. The fertilized ova are held in the reproductive tract usually for several months until environmental conditions are favorable to begin development.

This reproductive strategy is used by the Australian sharpnose shark, *Rhizoprionodon taylori* (Simpfendorfer, '92), the lesser electric ray, *Narcine brasiliensis* (Villavicencio-Garayzar, '93), and the bluntnose stingray, *Dasyatis sayi* (Snelson et al., '89). Lewis ('82) indicates that fertilization occurs anterior to the nidamental gland in *D. sabina*. In the documented cases of arrested development, fertilized but undeveloped ova are observed in the reproductive tract or uterus for several months prior to embryonic development. *D. sabina* uteri examined from October 1994 through March 1995 contained no ova released from the ovary or held in the reproductive tract. Released ova are observed only at ovulation in March–April, followed by fertilization and development in the uterus over subsequent summer months. Thus, continuous development of oocytes, lack of fertilized but undeveloped eggs in the uterus, and immediate embryonic development following ovulation in *D. sabina* makes arrested development unlikely.

Reproductive induction hypothesis

Hormonal control of sexual development and behavior is well documented in several elasmobranch species (Sumpter and Dodd, '79; Rasmussen et al., '92; Wright and Demski, '93). Environmental cues such as temperature and photoperiod control the endocrine regulation of spermatogenesis in the catshark, *S. canicula* (Dobson and Dodd, '77b). Thus, the onset of spermatogenic activity in male *D. sabina* after mid-August is likely triggered by such environmental cues. The subsequent development of testicular tissue results in production of androgens and other steroid hormones. Male GSI reaches a maximum in October. This increased testicular biomass and associated increase in steroid-producing cells may coincide with elevated androgen levels responsible for the initiation of the aggressive and protracted male mating behavior in the fall.

Male vertebrates often control female reproductive receptivity through some form of precopulatory behavior (Walton, '55). Male stingray reproductive behavior is likely initiated by the release in summer months of gonadotropins (luteinizing and follicle-stimulating-like hormones) that target the gonad and promote testis recrudescence and steroid hormone production. Elevated androgens elicit aggressive behavior in male fishes (Hoar, '69) and thus may directly activate male precopulatory biting and copulation with females. The coincidence of mating activity and onset of oocyte growth in September–October leads to the question of whether the latter is initiated by endogenous or environmental cues, or possibly induced by male biting and copulation. Female steroid concentrations increase during mating and oocyte maturation for several elasmobranch species (Rasmussen, '92; Manire et al., '95). Thus, the onset of mating activity in the fall in *D. sabina* may induce steroid production and/or ova development in females, and not function to provide sperm for fertilization.

Induced ovulation occurs in several vertebrate species where copulatory activity is necessary for the release of ova (Pearson, '44; Enders, '52). Ovulation and fertilization in *D. sabina* occur in a narrow time window between mid-March and mid-April. Sperm in the female reproductive tract, mating scars, and enlarged seminal vesicles in males indicate that mating activity is still in progress at this time. Thus, unlike in the fall, mating activity in March–April may function to induce female ovulation and provide viable sperm for fertilization.

The consideration that ovulation is not induced by copulation and the possibility of multiple phenomena responsible for the protracted mating period must also be addressed. Several additional (and noninclusive) hypotheses are proposed to explain this protracted mating: (1) protracted mating may function for postcopulatory sperm competition in which males with the largest total sperm production are likely to fertilize the most eggs, (2) mating at the time of ovulation may represent intrasexual competition among males in which females are fertilized by the fittest males, and (3) the early fall and winter mating activity may be a result of aggressive male behavior driven by elevated steroid hormones necessary for testis development and directed upon females that remain in a prime feeding habitat without refuge from males. Analysis of serum steroid concentrations is in progress for animals used in this study and may provide valuable information necessary to understand the regulation and timing of reproductive events and behavior in this species.

This paper is dedicated to the many volunteers and graduate students who have assisted in collections and data acquisition over the years.

LITERATURE CITED

Abdel-Aziz, S.H. (1994) Observations on the biology of the common torpedo (*Torpedo torpedo*, Linnaeus, 1758) and marbled electric ray (*Torpedo marmorata*, Risso, 1810) from Egyptian Mediterranean waters. Aust. J. Mar. Fresh. Res., *45*:693–704.

Babel, J.S. (1967) Reproduction, life history, and ecology of the round stingray, *Urolophus halleri* Cooper. Fish. Bull., *137*:3–103.

Cook, D.A. (1994) Temporal patterns of food habits of the Atlantic stingray, *Dasyatis sabina* (LeSeur, 1824), from the Banana River Lagoon, Florida. Thesis, Florida Institute of Technology, Melbourne.

Craik, J.C.A. (1978) An annual cycle of vitellogenesis in the elasmobranch *Scyliorhinus canicula*. J. Mar. Biol. Assoc. U.K., *58*:719–726.

Di Giacomo, E.E., and M.R. Perier (1994) Reproductive biology of the cockfish, *Callorhynchus callorhynchus* (Holocephali: Callorhynchidae) in Patagonian waters (Argentina). Fish. Bull., *92*:531–539.

Dobson, S. (1974) Endocrine control of reproduction in the male *Scyliorhinus canicula*. Ph.D. Dissertation, University of Wales.

Dobson, S., and J.M. Dodd (1977) The role of temperature and photo period in the response of the testis of the dogfish, *Scyliorhinus canicula*, L. to partial hypophysectomy (ventral lobectomy). Gen. Comp. Endocrinol., *32*:114–115.

Dodd, J.M. (1972) Ovarian control in cyclostomes and elasmobranchs. Am. Zool., *12*:325–339.

Enders, R.K. (1952) Reproduction in the mink (*Mustela vison*). Proc. Am. Philos. Soc., *96*:691–755.

Gilmore, G.R. (1993) Reproductive biology of lamnoid sharks. Environ. Biol. Fish., *38*:95–114.

Grier, H.J. (1992) Chordate testis: The extracellular matrix hypothesis. J. Exp. Zool., *261*:151–160.

Grier, H.J. (1993) Comparative organization of Sertoli cells including the Sertoli cell barrier. In: The Sertoli Cell. L.D. Russell and M.D. Griswold, eds. Cache River Press, Clearwater, FL, pp. 703–739.

Hoar, W.S. (1969) Reproduction. In: Fish Physiology. W.S. Hoar and D.J. Randall, eds. Academic Press, New York, vol.3, pp. 1–72.

Howarth, B. Jr. (1974) Sperm storage: As a function of the female reproductive tract. In: The Oviduct and Its Functions. A.D. Johnson and C.W. Foley, eds. Academic Press, New York, pp. 237–270.

Humason, G.L. (1979) Animal Tissue Techniques. Fourth edition. W.H. Freeman and Company, San Francisco.

Lewis, T.C. (1982) The reproductive anatomy, seasonal cycles, and development of the Atlantic stingray, *Dasyatis sabina* (Lesueur) (Pisces, Dasyatidae) from the northeastern Gulf of Mexico. Ph.D. Dissertation, Florida State University, Tallahassee.

Manire, C.H., L.E.L. Rasmussen, D.L. Hess, and R.E. Hueter (1995) Serum steroid hormones and the reproductive cycle of the female bonnethead shark, *Sphyrna tiburo*. Gen. Comp. Endocrinol., *97*:366–376.

Matthews, L.H. (1950) Reproduction in the basking shark, *Cetorhinus maximus* (Gunner). Philos. Trans. R. Soc. Lond., *234*:247–316.

Metten, H. (1944) The fate of spermatozoa in the female dogfish (*Scyliorhinus canicula*). Q. J. Microsc. Sci., *84*:283–295.

Parsons, G.R. (1982) The reproductive biology of the Atlantic sharpnose shark, *Rhizoprionodon terraenovae*. Fish. Bull. U.S., *81*:61–73.

Parsons, G.R., and H.J. Grier (1992) Seasonal changes in shark testicular structure and spermatogenesis. J. Exp. Zool., *261*:173–184.

Pearson, O.P. (1944) Reproduction in the shrew (*Blarina brevicauda* Say). Am. J. Anat., *75*:39–93.

Peres, M.B., and C.M. Vooren (1991) Sexual development, reproductive cycle, and fecundity of the school shark *Galeorhinus galeus* off Southern Brazil. Fish. Bull., *89*:655–667.

Pratt, H.L. (1988) Elasmobranch gonad structure: A description and survey. Copeia, *3*:719–729.

Pratt, H.L. (1993) The storage of spermatozoa in the oviducal glands of western North Atlantic sharks. Environ. Biol. Fish., *38*:139–149.

Pratt, H.L., and S. Tanaka (1994) Sperm storage in male elasmobranchs: A description and survey. J. Morphol., *219*:297–308.

Rasmussen, L.E.L., D.L. Hess, and S.H. Gruber (1992) Serum steroid hormones during reproduction in elasmobranchs. In: Reproductive Biology of South American Vertebrates. W.C. Hamlett, ed. Springer-Verlag, New York, pp. 19–42.

Simpfendorfer, C.A. (1992) Reproductive strategy of the Australian sharpnose shark, *Rhizoprionodon taylori* (Elasmobranchii: Carcharhinidae), from Cleveland Bay, Northern Queensland. Aust. J. Mar. Freshwater Res., *43*:67–75.

Simpson, T.H., and C.S. Wardle (1967) A seasonal cycle in the testis of the spurdog, *Squalus acanthias*, and the sites of 3, beta-hydroxysteroid dehydrogenase activity. J. Mar. Biol. Assoc. U.K., *47*:699–708.

Snelson, F.F., S.E. Williams-Hooper, and T.H. Schmid (1988) Reproduction and ecology of the Atlantic stingray, *Dasyatis sabina*, in Florida coastal lagoons. Copeia, *3*:729–739.

Snelson, F.F., S.E. Willams-Hooper, and T.H. Schmid (1989) Biology of the bluntnose stingray, *Dasyatis sayi*, in Florida coastal lagoons. Bull. Mar. Sci., *45*:15–25.

Sumpter, J.P., and J.M. Dodd (1979) The annual reproductive cycle of the female lesser spotted dogfish, *Scyliorhinus canicula* L., and its endocrine control. J. Fish. Biol., *15*:687–695.

Tanaka, S., Y. Shiobara, S. Hioki, H. Abe, G. Nishi, K. Yano, and K. Suzuki (1990) The reproductive biology of the frilled shark, *Chlamydoselachus anguineus*, from Suruga Bay, Japan. Jap. J. Ichthyol., *37*:273–300.

Teshima, K. (1981) Studies on the reproduction of the Japanese smooth dogfishes, *Mustelus manazo* and *Mustelus griseus*. J. Shimonoseki Univ. Fish., *29*:113–199.

Villavicencio-Garayzar, C.J. (1993) Observaciones sobre la biologia reproduction de *Narcine brasiliensis* (Olfers) (Pisces: Narcinidae), en Bahia Almejas B.C.S. Mexico. Rev. Inv. Cient., *4*:95–99.

Walton, A. (1955) Sexual Behavior. In: Progress in the Physiology of Farm Animals. J. Hammond, ed. Butterworth and Company, London, pp. 603–616.

Wourms, J.P. (1977) Reproduction and development in chondrichthyan fishes. Am. Zool., *17*:379–410.

Wright, D.E., and L.S. Demski (1993) Gonadotropin-releasing hormone (GnRH) pathways and reproductive control in elasmobranchs. Environ. Biol. Fish., *38*:209–218.